JSHC
Japan Society of
Histochemistry and Cytochemistry
Established 1959

Acta Histochem. Cytochem. 44 (5): 223–231, 2011
doi:10.1267/ahc.11030

Autophagy Is Constitutively Active in Normal Mouse Sino-Atrial Nodal Cells

Mariko Omatsu-Kanbe[1], Takefumi Yamamoto[2] and Hiroshi Matsuura[1]

[1]Department of Physiology, Shiga University of Medical Science and [2]Central Research Laboratory, Shiga University of Medical Science, Otsu, Shiga 520–2192, Japan

Received June 16, 2011; accepted July 7, 2011; published online August 10, 2011

This study was designed to examine the autophagy in sino-atrial (SA) nodal cells from the normal adult mouse heart. Autophagy is the cellular process responsible for the degradation and recycling of long-lived and/or damaged cytoplasmic components by lysosomal digestion. In the heart, autophagy is known to occur at a low level under physiological conditions, but to become upregulated when cells are exposed to certain stresses, such as ischemia. We examined whether the basal level of autophagy in SA nodal cells was different from that in ventricular or atrial myocytes. An ultrastructural analysis revealed that the SA nodal cells contained a number of autophagic vacuoles (autophagosomes) with various stages of degradation by lysosomal digestion, whereas the number of those in ventricular or atrial myocytes was either negligible or very small. The immunostaining of autophagosome marker microtubule-associated protein 1 light chain 3 (LC3) and lysosome marker lysosome-associated membrane protein 1 (LAMP1) indicated that the content of both autophagosomes and lysosomes were much greater in SA nodal cells than in ordinary cardiomyocytes. Our results provide evidence that the autophagy is active in normal SA nodal cells, which is not a stress-activated process but a constitutive event in the mouse heart.

Key words: autophagy, SA node, cardiomyocyte, LC3, LAMP1

I. Introduction

Autophagy is a conserved process for the degradation of long-lived and/or damaged proteins and organelles [13, 15, 16]. In this process, cellular constituents are sequestered within double- or multi-membraned autophagic vacuoles, named autophagosomes, which subsequently fuse with lysosomes for bulk degradation and recycling. Autophagy plays a role not only in cell death, but also in survival under nutrient-deprived conditions. It has been demonstrated in the heart that autophagy is activated in response to various stresses, such as ischemia/reperfusion [6, 8, 19] and heart failure [30]. Under physiological conditions in the heart, autophagy remains at a low level and plays a role in the maintenance of the cells [22, 24]. During the neonatal period, autophagy provides a necessary source of energy by the degradation of self-proteins in various tissues including the heart [14].

The sino-atrial (SA) node, first established as the origin of the cardiac impulse conduction system in 1907 [12], exhibits specialized morphological and electrophysiological properties distinct from other cardiac myocytes. Electrophysiological studies revealed that the central part of the SA node was responsible for generating the electrical impulse for the regular and rhythmic contraction of the heart [1]. In morphological studies, the cardiomyocytes within the SA node are generally classified as central nodal cells in the center of the node, and peripheral nodal cells surrounding the central nodal cells. The peripheral nodal cells are further distinguished into two cell types: transitional cells close to the central nodal cells and atrial cells at the border of the peripheral zone into the atrial myocytes [2]. Ultrastructural studies of the SA node have usually focused on the organelles and proteins that play a role in both the pacemaker activity and cell-to-cell coupling [1, 10, 18, 26], as well as electrophysiological studies focused on the regulation of the automaticity [17, 20, 32].

Correspondence to: Mariko Omatsu-Kanbe, Ph.D., Department of Physiology, Shiga University of Medical Science, Tsukinowa-cho, Seta, Otsu, Shiga 520–2192, Japan.
E-mail: m_omatsu@belle.shiga-med.ac.jp

The aim of the present study was to examine the level of autophagy in the SA nodal cells. Our results show that the basal activity of autophagy in the nodal cells is much higher than that in ventricular or atrial myocytes in normal adult mouse heart.

II. Materials and Methods

Animal and tissue preparation

Male C57BL/6J mice (Charles River Japan, Yokohama) aged 8–12 weeks were used for the experiments. All animal experiments were performed in accordance with the guidelines of the institution's Animal Care and Use Committee.

The animals were killed by an intraperitoneal injection of a mixture of sodium pentobarbital overdose (>300 mg/kg) and heparin (8000 U/kg). The heart was quickly excised and retrogradely perfused [31] at 37°C for 3 min with Tyrode solution containing (in mM) 140 NaCl, 5.4 KCl, 1.8 $CaCl_2$, 0.5 $MgCl_2$, 0.33 NaH_2PO_4, 5.5 glucose and 5.0 HEPES (pH adjusted to 7.4 with NaOH) to discharge blood. Both ventricles were then cut out and fixed in 4% formaldehyde in PBS.

To isolate the atria, the heart was retrogradely perfused at 37°C for 6 min with an enzyme solution containing 0.1% collagenase, 0.006% trypsin and 0.006% protease in a solution containing (in mM) 130 NaCl, 5.4 KCl, 0.5 $MgCl_2$, 0.33 NaH_2PO_4, 22 glucose, 50 μU/mL bovine insulin, and 25 HEPES (pH adjusted to 7.4 with NaOH) [25]. The left atrium was excised and fixed in 4% formaldehyde. The SA node region, bordered by the crista terminalis, the intra-atrial septum and the superior and inferior vena cava, was isolated from the right atrium under a microscope and fixed in 4% formaldehyde.

Electron microscopy

The heart tissues fixed with formaldehyde for 1–2 days at 4°C were further fixed with 2.5% glutaraldehyde in PBS for 30 min at 4°C and washed twice with PBS for 3 min, and then finally fixed with 2% osmium tetroxide for 30 min at 4°C. The fixed tissues were washed twice with PBS for 3 min at room temperature. The tissues were then dehydrated by immersion in a series of diluted ethanol, exchanged by immersion in a series of propylene oxide, and embedded in epoxy resin (EPON 812 resin embedding kit, TAAB, UK). After polymerization for 6 hr at 60°C, the areas of interest were cut from the samples, and 70 nm ultra-thin sections were made using an Ultracut E ultramicrotome (Reichert-Jung, Austria). The ultra-thin sections were mounted on 200 mesh nickel thin bar grids (Gilder Grids, UK). The grids were stained with 2% uranyl acetate and lead stain solution (Sigma-Aldrich), and then observed with a Hitachi 7500 electron microscope (Tokyo).

Antibodies

The primary antibodies used were: rabbit polyclonal anti-microtubule-associated protein 1 light chain 3 (anti-LC3, Medical & Biological Laboratories, Nagoya), anti-lysosome-associated membrane protein 1 (anti-LAMP1, Abcam, U.K.), anti-mammalian target of rapamycin (anti-mTOR, Abcam) and anti-phosphorylated mTOR at Ser2448 (anti-mTOR-phospho S2488, Abcam) antibodies. The secondary antibody was Alexa Fluor® 488-conjugated anti-rabbit IgG (Molecular Probes-Invitrogen, USA).

Immunostaining

The heart tissues fixed with 4% formaldehyde in PBS for 3 days at 4°C were embedded in paraffin. Then, 4 μm paraffin sections were deparaffinized by xylene, rehydrated in a series of 100-70% ethanol and subjected to heat-mediated antigen retrieval according to the manufacturer's instructions for the antibodies, if necessary. The sections were blocked with 0.1% Triton X-100 and 10% BSA in PBS for 1 hr, incubated with anti-LC3 (1:1000), anti-LAMP1 (1:100), anti-mTOR (1:75) or anti-mTOR-phospho S2488 (1:75) for 1 hr, and rinsed with PBS. The sections were then incubated with secondary antibody (1:1000), rinsed with PBS and mounted with glass cover slips in a 1:1 solution of glycerol and PBS. All procedures were performed at room temperature. Nuclei were stained with 4'-6-diamino-2-phenylindole (DAPI). Fluorescent signals were analyzed using a confocal laser scanning system C1si on an Eclipse TE2000-E inverted microscope (Nikon, Tokyo). Each image acquired by C1si was 1024×1024 pixels (318.25×318.25 or 636.5×636.5 μm with a ×40 or ×20 objective, respectively) in size.

The anti-LC3 antibody used for the present study reacts with both cytosolic LC3-I and autophagosome-associated membrane-bound LC3-II. Therefore, dotted fluorescent signals (intensity≥55 of 255 gradation) were counted as autophagosome-associated membrane-bound LC3, and uniformly distributed fluorescent signals (intensity<55 of 255 gradation) were estimated as cytosolic LC3. Since cardiomyocytes often possess two nuclei and the myocardium contains non-myocyte cells, the number of DAPI-stained nuclei did not reflect the exact number of cardiomyocytes. In the present study, the area of the membrane-bound fluorescent signals (μm^2) per 10 nuclei calculated by a computer using the Image-Pro Plus software program (Media Cybernetics Inc., USA) was estimated as the averaged immunofluorescent signals for membrane-bound LC3. The data are expressed as the means±S.E.M. from three mice (n=3) and each value was the average of five different images.

Statistical analyses

Statistical comparisons were made using one-way ANOVA followed by Tukey's test, and differences were considered to be significant at $P<0.001$.

III. Results

The electron micrographs of a normal mouse cardiac ventricle (Fig. 1A) and atrium (Fig. 1B) demonstrated well-organized myofibers and a large number of mitochondria.

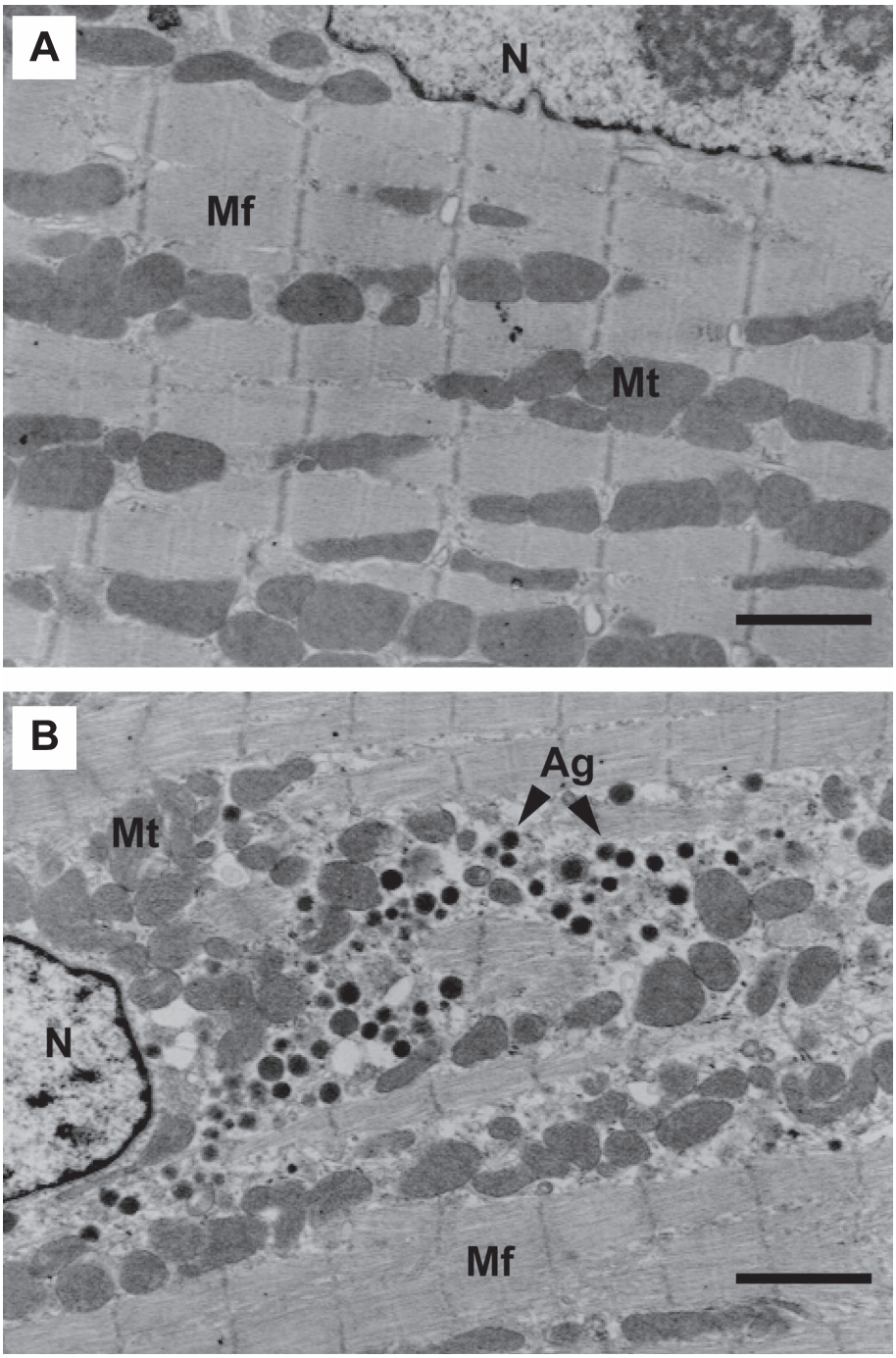

Fig. 1. Ultrastructure of the adult mouse myocardium. Electron micrographs of the cardiac ventricle (**A**) and left atrium (**B**). N, nucleus; Mt, mitochondria; Mf, myofiber. The arrowheads indicate atrial granules (Ag). The right atrium of the mouse was used for the preparation of the SA node (see Fig. 2). Bar=1.7 μm.

Atrial natriuretic peptide (ANP)-containing secretory granules, known as atrial granules, were also observed in the ultra-thin sections of the atrium, as expected [3, 5]. In contrast to the ordinary cardiac muscle cells, the ultrastructure of SA nodal cells demonstrate a low amount of myofibers, running in every direction (Fig. 2A), and numerous pinocytotic vesicles invaginated from the plasma membrane (Fig. 2B, arrowheads), thus indicating the features of the central nodal cells [1, 2, 10, 18].

It is noted that SA nodal cells contain various sizes of vacuoles throughout the entire cell space, including the perinuclear area, interspaces among myofibers, and the cell periphery (Fig. 2), while the distributions of vacuoles in whole cells were not commonly observed in normal ventricular or atrial myocytes (Fig. 1). The observation of a number of vacuoles in the cytoplasmic space usually

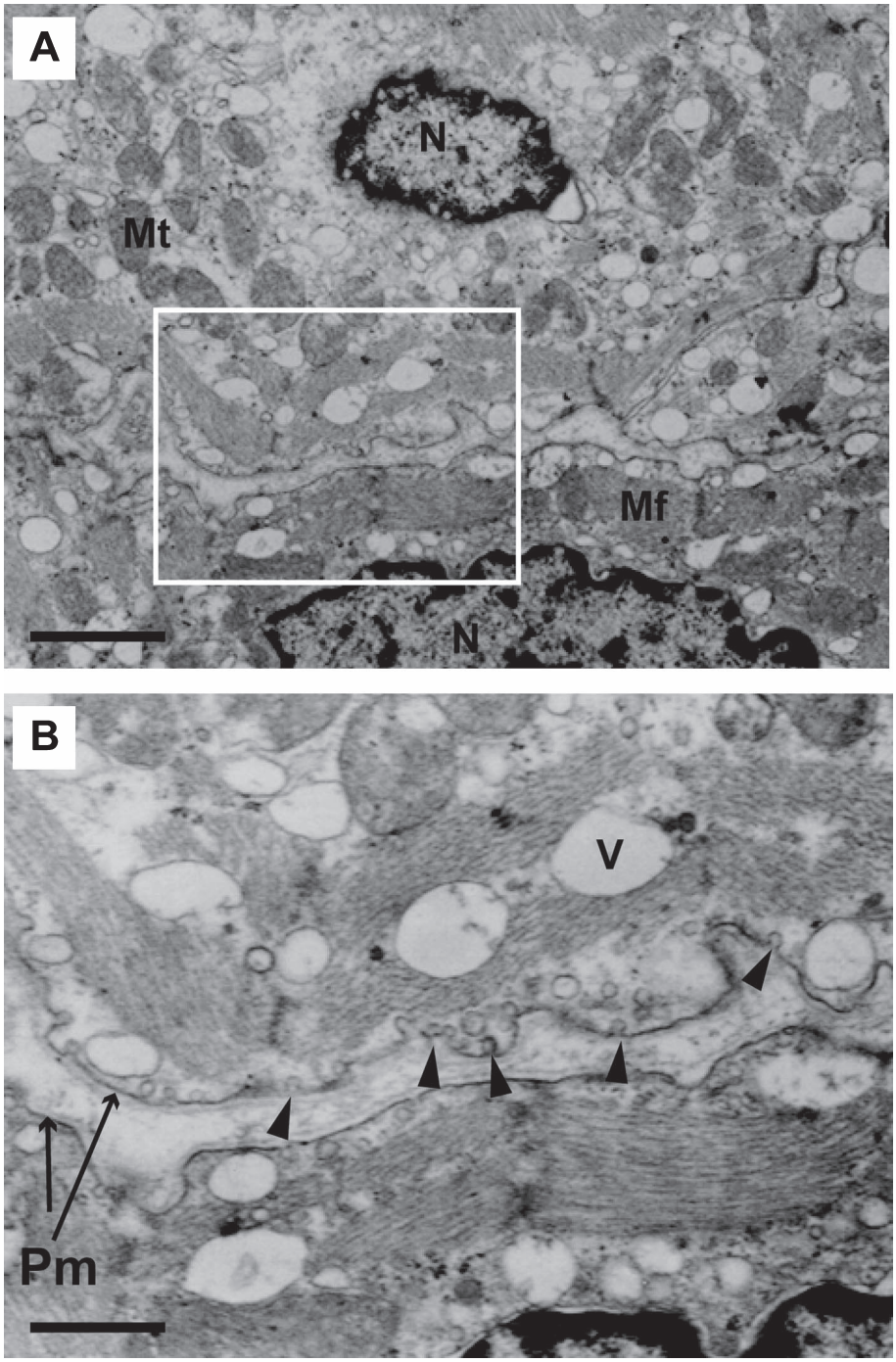

Fig. 2. Ultrastructure of the adult mouse SA node. (**A**) Electron micrographs of the SA node. The area marked in white is enlarged in (**B**). N, nucleus; Mt, mitochondria; Mf, myofiber; V, vacuole; Pm, plasma membrane. The arrowheads indicate pinocytotic vesicles. Bars=1.7 μm (**A**) and 667 nm (**B**).

suggests the upregulation of autophagy in the cells [13, 16].

A number of autophagosomes were identified in the SA nodal cells (Fig. 3, arrows), such as the space near the neural components (Fig. 3A), perinucleus (Fig. 3B), and periphery (Fig. 3C, D), displaying various stages of degradation by lysosomal digestion. The residual bodies with typical myelin-like figures (Fig. 3D) indicated that the trapped organelles, mostly mitochondria, were degraded, except for the membrane-bound indigestible remnants. In addition, sequestering of cytoplasmic components by a double-membrane was also observed in the perinuclear area (Fig. 3E, arrows), thus suggesting that proteins and/or cytoplasm are also degraded via autophagy.

Microtubule-associated protein 1 light chain 3 (LC3),

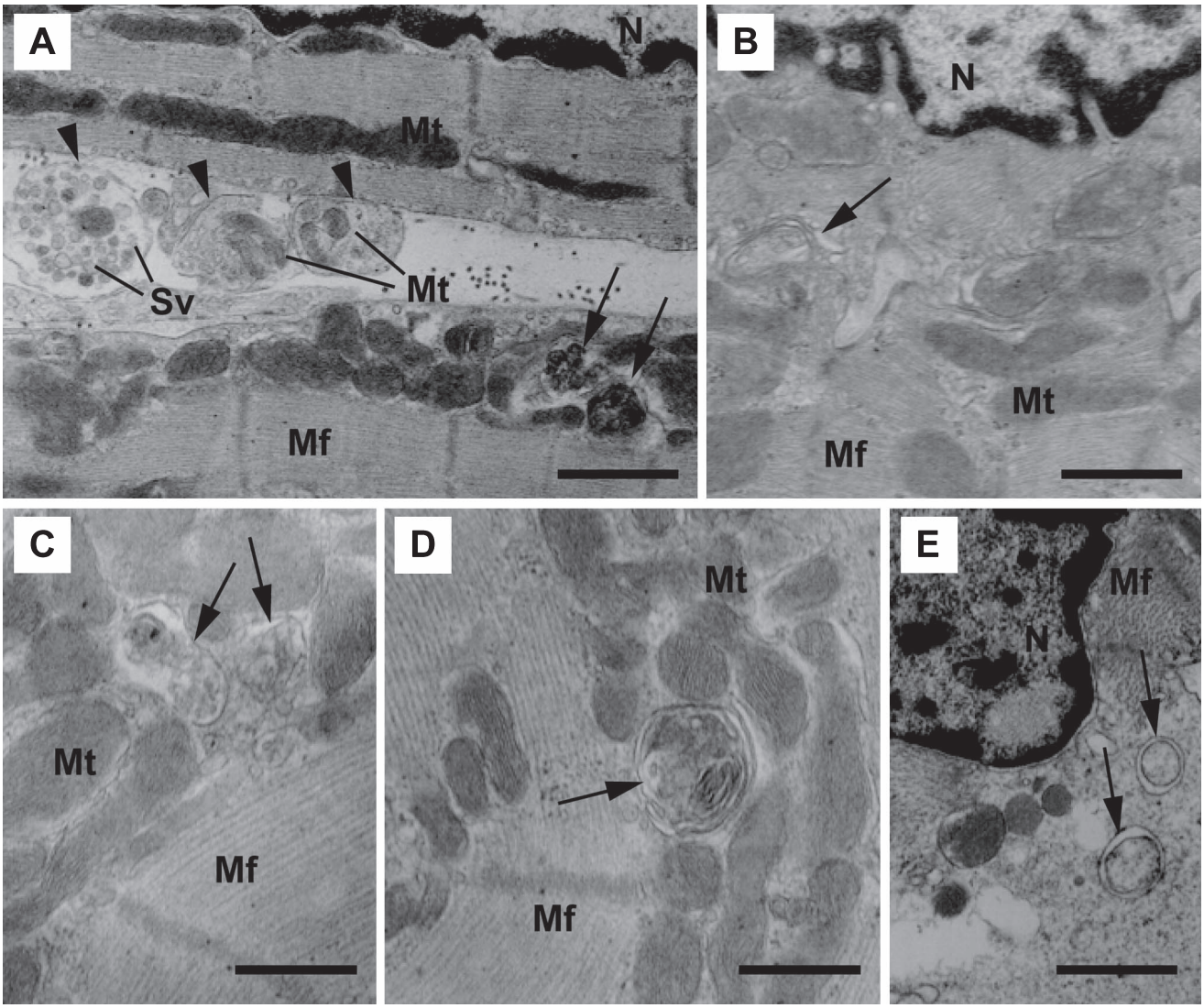

Fig. 3. Autophagosomes in SA nodal cells. Electron micrographs of SA nodal cells, including autophagosomes (arrows). N, nucleus; Mt, mitochondria; Mf, myofiber. The arrowheads (**A**) indicate nerve terminals containing synaptic vesicles (Sv) and small mitochondria. Bars=1 μm (**A, B, E**) and 500 nm (**C, D**).

a homologue of yeast Apg8p, is essential for autophagy, and two forms of LC3, cytosolic LC3-I and autophagosome-associating membrane-bound LC3-II, are post-translationally produced in various cells [11]. In the normal heart, the area of immunofluorescent signals for the estimated membrane-bound LC3 were relatively low in ventricles (3.33±1.63 μm^2/10 nuclei) and in atria (16.51±7.22 μm^2/10 nuclei) but was extremely high in SA nodes (899.51±99.84 μm^2/10 nuclei, Fig. 4). In the enlarged image of SA node, dotted fluorescent signals for membrane-bound LC3 were clearly observed within the cells (Fig. 4). These observations indicate that the number of autophagosomes in the SA node was much higher than that in the ordinary cardiomyocytes.

Lysosome associated membrane protein 1 (LAMP1) is known to be one of the major protein components of the lysosomal membrane [4] and used for the marker of the lysosomal localization [21]. The distribution of immunofluorescent signals for LAMP1 in the heart tissue indicated that lysosomes were scattered in ventricular and atrial myocytes, whereas the accumulation of lysosomes were observed in the perinuclear and also peripheral spaces in SA nodal cells (Fig. 5), which suggest that the functions of lysosomes are more active in SA nodal cells compared to those in the other cardiomyocytes. These observations show that autophagy is active in normal SA nodal cells, but not in ordinary cardiomyocytes.

Autophagy is negatively regulated by mammalian target of rapamycin (mTOR) [16, 28, 29, 33]. It has been known that the function of mTOR is activated by the phosphorylation at Ser 2448 [9, 23, 27]. The immunostaining analyses revealed that the phosphorylated mTOR at Ser 2448 can be detected in normal SA node, as well as in ventricle and atrium (Fig. 6), suggesting that the autophagy in the normal SA nodal cells is not likely due to the inactivation of mTOR.

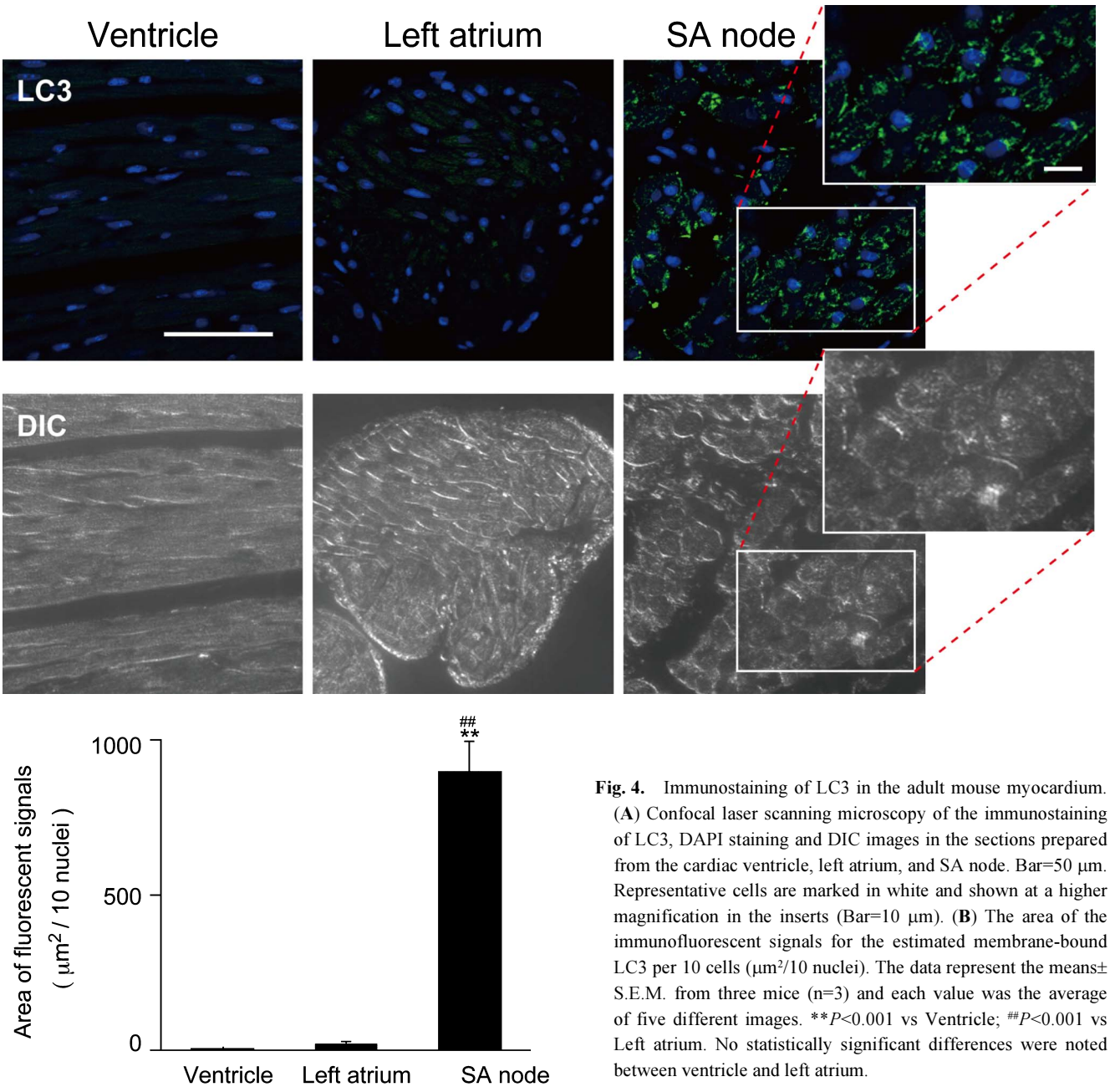

Fig. 4. Immunostaining of LC3 in the adult mouse myocardium. (**A**) Confocal laser scanning microscopy of the immunostaining of LC3, DAPI staining and DIC images in the sections prepared from the cardiac ventricle, left atrium, and SA node. Bar=50 μm. Representative cells are marked in white and shown at a higher magnification in the inserts (Bar=10 μm). (**B**) The area of the immunofluorescent signals for the estimated membrane-bound LC3 per 10 cells (μm²/10 nuclei). The data represent the means± S.E.M. from three mice (n=3) and each value was the average of five different images. $^{**}P<0.001$ vs Ventricle; $^{\#\#}P<0.001$ vs Left atrium. No statistically significant differences were noted between ventricle and left atrium.

IV. Discussion

SA nodal cells have been known as "primitive cardiomyocytes" because of their empty appearance on micrographs, mostly related to their poor development of myofibers. These characteristics are more apparent in central nodal cells, whereas peripheral nodal cells are more similar to the atrial myocytes [2].

Another morphological characteristic specifically observed in SA nodal cells, but not in other cardiomyocytes, is a large number of membrane vesicles invaginated from the plasma membrane, especially in central nodal cells (Fig. 2) [10, 18]. The presence of these membrane vesicles indicates that pinocytosis is highly activated in SA nodal cells, because all of the vesicles are positive for the extracellular marker, even when not connected to the plasma membrane [18]. Pinocytosis is an energy-dependent event and primarily occurs during the non-specific absorption of extracellular fluid, including electrolytes and nutrients. However, the particular role of pinocytosis in SA nodal cells is unclear. Ion channels in the plasma membrane in cardiomyocytes have been demonstrated to internalize and recycle quickly; for example, the voltage-gated potassium channel, $K_V1.5$, that is expressed in the SA nodal pacemaker cells [7], recycles within 2 hr or so [34]. Since the membrane proteins recycle through a vesicle trafficking pathway similar to the pinocytotic pathway, it is likely that the pinocytosis occurs in ion channel-rich areas of the plasma membrane,

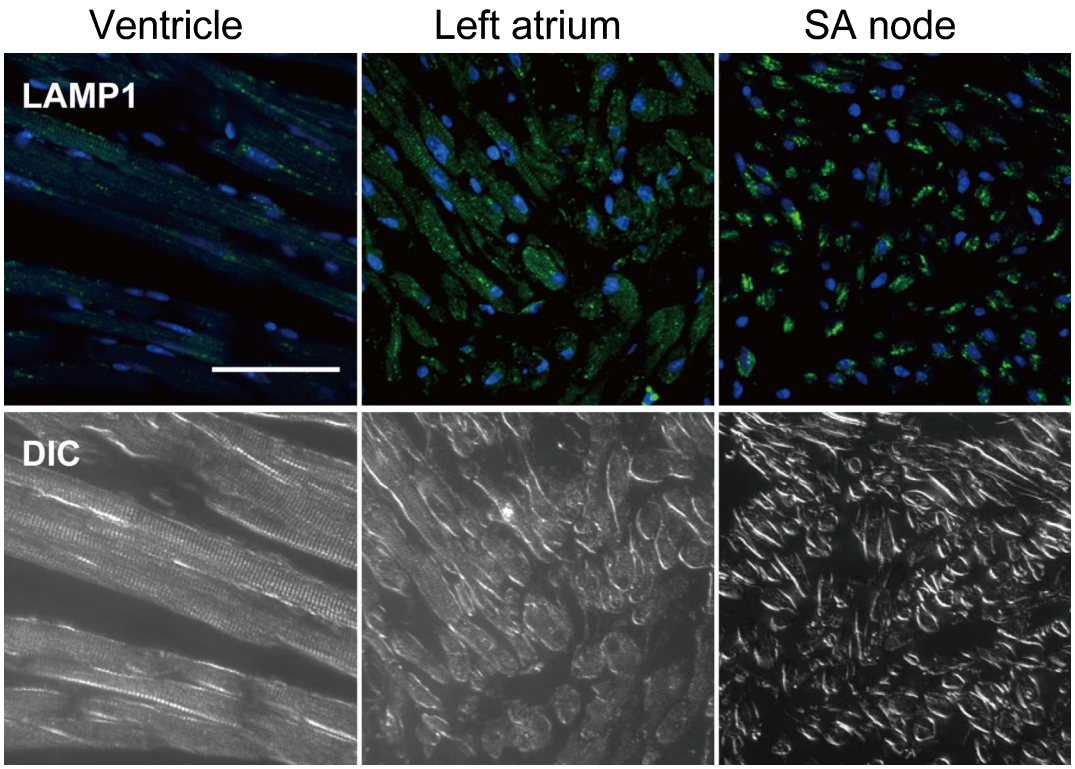

Fig. 5. Immunostaining of LAMP1 in the adult mouse myocardium. Confocal laser scanning microscopy of the immunostaining of LAMP1, DAPI staining and DIC images in the sections prepared from cardiac ventricle, left atrium and SA node. Bar=50 μm.

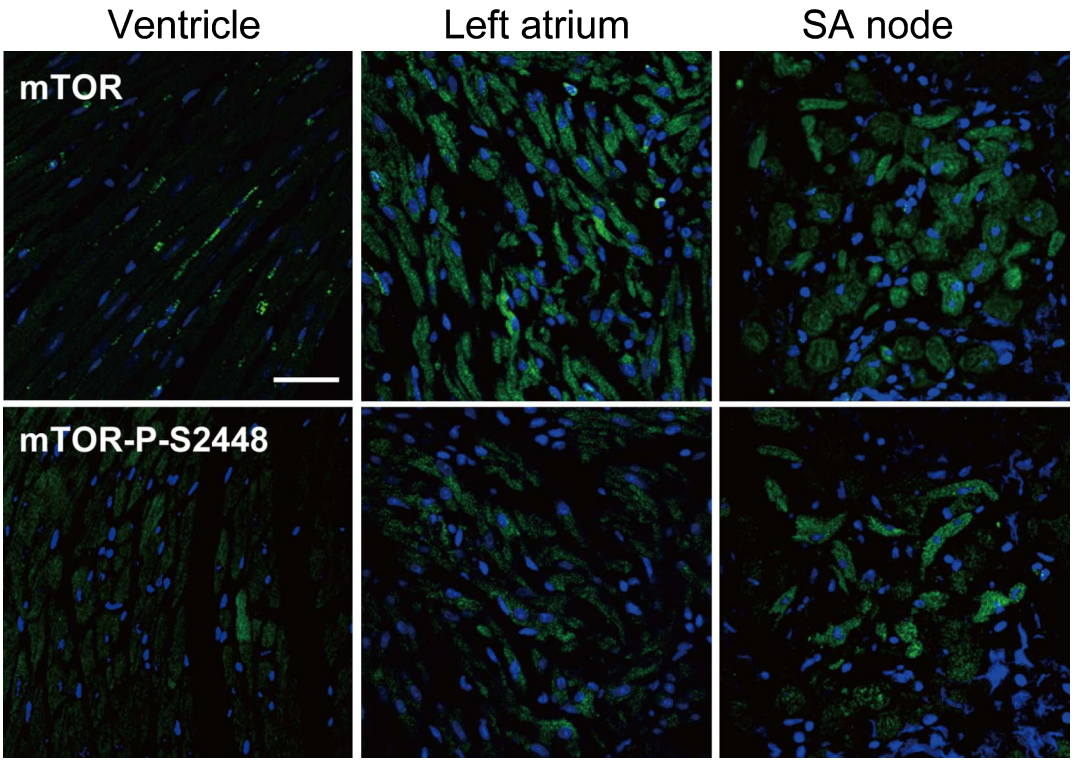

Fig. 6. Immunostaining of mTOR and phosphorylated mTOR in the adult mouse myocardium. Confocal laser scanning microscopy of the immunostaining of mTOR or phosphorylated mTOR at Ser2448 residue (mTOR-P-S2448) and DAPI staining in the sections prepared from cardiac ventricle, left atrium and SA node. Bar=50 μm.

such as the caveolae, thus contributing to, at least in part, the rapid recycling of the channel proteins in SA nodal cells.

The evidence that the SA nodal cells, but not ventricular or atrial myocytes, contain a number of autophagosomes in various stages of degradation (Fig. 3), membrane-bound LC3 (Fig. 4), and accumulated lysosomes (Fig. 5) indicates that the autophagy in the SA node is not a stress-activated process, but a constitutive event, at least in the mouse heart. Autophagosomes were identified in nodal cells containing a low amount of myofibers running in different directions (Fig. 3B, C, E) and those cells containing relatively organized myofibers (Fig. 3A, D). Furthermore, immunofluorescent signals of membrane-bound LC3 were observed in a whole image of the SA node (Fig. 4). These observations suggest that autophagy is active in both central and peripheral nodal cells. Quantitative analyses of the local autophagy within the SA node will therefore be the focus of future studies. Autophagy is induced by various factors including mTOR-dependent and -independent enhancers [28]. The observation that the phosphorylation of mTOR at Ser 2448 is clearly detected in SA nodal cells (Fig. 6) suggests the possibility that the constitutively active autophagy is regulated somewhat by mTOR-independent pathway in normal SA nodal cells.

The autophagy in the heart, mainly in the ventricles, has been examined to elucidate its cardio-protective and/or self-destructive role under pathophysiological conditions [6, 8, 19, 22, 24, 30], and such studies have indicated that the basal level of autophagy is low in the myocardium. Those data suggest that the rhythmic contractions are not "autophagy-inducible stresses" to the cardiomyocytes under physiological conditions. The precise mechanism of the relatively high level of autophagy in normal SA nodal cells is unclear. It is possible that this autophagy may produce amino acids by degradation of self-proteins to supply a sufficient energy source for active vesicle trafficking, including pinocytosis and ion channel recycling, in addition to the pacemaker activity in SA nodal cells. Further studies are required to explore whether the high basal level of autophagy is necessary for the basal maintenance of SA nodal cells.

V. Acknowledgments

We wish to thank Professor Hiroyuki Sugihara, Department of Pathology, Shiga University of Medical Science, for his helpful suggestions. This work was supported in part by Grants-in-Aid for Scientific Research from the Japan Society for the Promotion of Science (No. 22590204 to MOK and No. 22590205 to HM).

VI. References

1. Bleeker, W. K., Mackaay, A. J., Masson-Pevet, M., Bouman, L. N. and Becker, A. E. (1980) Functional and morphological organization of the rabbit sinus node. *Circ. Res.* 46; 11–22.
2. Bouman, L. N. and Jongsma, H. J. (1986) Structure and function of the sino-atrial node: a review. *Eur. Heart J.* 7; 94–104.
3. Chapeau, C., Gutkowska, J., Schiller, P. W., Milne, R. W., Thibault, G., Garcia, R., Genest, J. and Cantin, M. (1985) Localization of immunoreactive synthetic atrial natriuretic factor (ANF) in the heart of various animal species. *J. Histochem. Cytochem.* 33; 541–550.
4. Chen, J. W., Murphy, T. L., Willingham, M. C., Pastan, I. and August, J. T. (1985) Identification of two lysosomal membrane glycoproteins. *J. Cell Biol.* 101; 85–95.
5. de Bold, A. J. (1985) Atrial natriuretic factor: a hormone produced by the heart. *Science* 230; 767–770.
6. Decker, R. S. and Wildenthal, K. (1980) Lysosomal alterations in hypoxic and reoxygenated hearts. I. Ultrastructural and cytochemical changes. *Am. J. Pathol.* 98; 425–444.
7. Dobrzynski, H., Rothery, S. M., Marples, D. D., Coppen, S. R., Takagishi, Y., Honjo, H., Tamkun, M. M., Henderson, Z., Kodama, I., Severs, N. J. and Boyett, M. R. (2000) Presence of the $K_v1.5$ K+ channel in the sinoatrial node. *J. Histochem. Cytochem.* 48; 769–780.
8. Hamacher-Brady, A., Brady, N. R. and Gottlieb, R. A. (2006) Enhancing macroautophagy protects against ischemia/reperfusion injury in cardiac myocytes. *J. Biol. Chem.* 281; 29776–29787.
9. Harasawa, M., Yasuda, M., Hirasawa, T., Miyazawa, M., Shida, M., Muramatsu, T., Douguchi, K., Matsui, N., Takekoshi, S., Kajiwara, H., Osamura, R. Y. and Mikami, M. (2011) Analysis of mTOR inhibition-involved pathway in ovarian clear cell adenocarcinoma. *Acta Histochem. Cytochem.* 44; 113–118.
10. James, T. N., Sherf, L., Fine, G. and Morales, A. R. (1966) Comparative ultrastructure of the sinus node in man and dog. *Circulation* 34; 139–163.
11. Kabeya, Y., Mizushima, N., Ueno, T., Yamamoto, A., Kirisako, T., Noda, T., Kominami, E., Ohsumi, Y. and Yoshimori, T. (2000) LC3, a mammalian homologue of yeast Apg8p, is localized in autophagosome membranes after processing. *EMBO J.* 19; 5720–5728.
12. Keith, A. and Flack, M. (1907) The form and nature of the muscular connections between the primary divisions of the vertebrate heart. *J. Anat. Physiol.* 41; 172–189.
13. Klionsky, D. J. and Emr, S. D. (2000) Autophagy as a regulated pathway of cellular degradation. *Science* 290; 1717–1721.
14. Kuma, A., Hatano, M., Matsui, M., Yamamoto, A., Nakaya, H., Yoshimori, T., Ohsumi, Y., Tokuhisa, T. and Mizushima, N. (2004) The role of autophagy during the early neonatal starvation period. *Nature* 432; 1032–1036.
15. Levine, B. and Klionsky, D. J. (2004) Development by self-digestion: molecular mechanisms and biological functions of autophagy. *Dev. Cell* 6; 463–477.
16. Maiuri, M. C., Zalckvar, E., Kimchi, A. and Kroemer, G. (2007) Self-eating and self-killing: crosstalk between autophagy and apoptosis. *Nat. Rev. Mol. Cell Biol.* 8; 741–752.
17. Mangoni, M. E. and Nargeot, J. (2001) Properties of the hyperpolarization-activated current I_f in isolated mouse sino-atrial cells. *Cardiovasc. Res.* 52; 51–64.
18. Masson-Pevet, M., Bleeker, W. K. and Gros, D. (1979) The plasma membrane of leading pacemaker cells in the rabbit sinus node. A qualitative and quantitative ultrastructural analysis. *Circ. Res.* 45; 621–629.
19. Matsui, Y., Takagi, H., Qu, X., Abdellatif, M., Sakoda, H., Asano, T., Levine, B. and Sadoshima, J. (2007) Distinct roles of autophagy in the heart during ischemia and reperfusion: roles of AMP-activated protein kinase and Beclin 1 in mediating autophagy. *Circ. Res.* 100; 914–922.
20. Matsuura, H., Ehara, T., Ding, W. G., Omatsu-Kanbe, M. and Isono, T. (2002) Rapidly and slowly activating components of delayed rectifier K^+ current in guinea-pig sino-atrial node pacemaker cells. *J. Physiol.* 540; 815–830.
21. Morioka, K., Sato-Kusubata, K., Kawashima, S., Ueno, T., Kominami, E., Sakuraba, H. and Hara, S. (2001) Localization of

cathepsin B, D, L, LAMP-1 and μ-calpain in developing hair follicles. *Acta Histochem. Cytochem.* 34; 337–347.
22. Nakai, A., Yamaguchi, O., Takeda, T., Higuchi, Y., Hikoso, S., Taniike, M., Omiya, S., Mizote, I., Matsumura, Y., Asahi, M., Nishida, K., Hori, M., Mizushima, N. and Otsu, K. (2007) The role of autophagy in cardiomyocytes in the basal state and in response to hemodynamic stress. *Nat. Med.* 13; 619–624.
23. Nave, B. T., Ouwens, M., Withers, D. J., Alessi, D. R. and Shepherd, P. R. (1999) Mammalian target of rapamycin is a direct target for protein kinase B: identification of a convergence point for opposing effects of insulin and amino-acid deficiency on protein translation. *Biochem. J.* 344; 427–431.
24. Nishida, K., Kyoi, S., Yamaguchi, O., Sadoshima, J. and Otsu, K. (2009) The role of autophagy in the heart. *Cell Death Differ.* 16; 31–38.
25. Omatsu-Kanbe, M., Yamamoto, T., Mori, Y. and Matsuura, H. (2010) Self-beating atypically shaped cardiomyocytes survive a long-term postnatal development while preserving the expression of fetal cardiac genes in mice. *J. Histochem. Cytochem.* 58; 543–551.
26. Opthof, T., de Jonge, B., Mackaay, A. J., Bleeker, W. K., Masson-Pevet, M., Jongsma, H. J. and Bouman, L. N. (1985) Functional and morphological organization of the guinea-pig sinoatrial node compared with the rabbit sinoatrial node. *J. Mol. Cell Cardiol.* 17; 549–564.
27. Ravikumar, B., Stewart, A., Kita, H., Kato, K., Duden, R. and Rubinsztein, D. C. (2003) Raised intracellular glucose concentrations reduce aggregation and cell death caused by mutant huntingtin exon 1 by decreasing mTOR phosphorylation and inducing autophagy. *Hum. Mol. Genet.* 12; 985–994.
28. Sarkar, S., Ravikumar, B., Floto, R. A. and Rubinsztein, D. C. (2009) Rapamycin and mTOR-independent autophagy inducers ameliorate toxicity of polyglutamine-expanded huntingtin and related proteinopathies. *Cell Death Differ.* 16; 46–56.
29. Schmelzle, T. and Hall, M. N. (2000) TOR, a central controller of cell growth. *Cell* 103; 253–262.
30. Shimomura, H., Terasaki, F., Hayashi, T., Kitaura, Y., Isomura, T. and Suma, H. (2001) Autophagic degeneration as a possible mechanism of myocardial cell death in dilated cardiomyopathy. *Jpn. Circ. J.* 65; 965–968.
31. Shioya, T. (2007) A simple technique for isolating healthy heart cells from mouse models. *J. Physiol. Sci.* 57; 327–335.
32. Verheijck, E. E., van Kempen, M. J., Veereschild, M., Lurvink, J., Jongsma, H. J. and Bouman, L. N. (2001) Electrophysiological features of the mouse sinoatrial node in relation to connexin distribution. *Cardiovasc. Res.* 52; 40–50.
33. Yorimitsu, T. and Klionsky, D. J. (2005) Autophagy: molecular machinery for self-eating. *Cell Death Differ.* 12; 1542–1552.
34. Zadeh, A. D., Xu, H., Loewen, M. E., Noble, G. P., Steele, D. F. and Fedida, D. (2008) Internalized $K_v1.5$ traffics via Rab-dependent pathways. *J. Physiol.* 586; 4793–4813.